PLANE DETECTION FROM MONOCULAR IMAGE SEQUENCES

Kelson R. T. Aires
DCA - UFRN
Natal, RN, Brazil
email: kelson@dca.ufrn.br

Helder de J. Araújo
ISR - DEEC - UC
Coimbra, Portugal
email: helder@isr.uc.pt

Adelardo A. D. de Medeiros
DCA - UFRN
Natal, RN, Brazil
email: adelardo@dca.ufrn.br

ABSTRACT

Planes are important geometric features and can be used in a wide range of applications. This work aims to illustrate a homography-based method to detect planes using the affine model. Using two image frames from a monocular sequence, a set of match pairs of interest points is obtained using Harris corner detector combined with the Scale Invariant Feature Transform (SIFT) as local descriptor. A Delaunay triangulation is performed on the set of detected corners of the first image and we use a triangle to calculate an affine homography that represents a plane in the image. An algorithm was developed to cluster interest points belonging to the same plane based on the reprojection error of the affine homography. Tests are performed in different sequences of indoor and outdoor images and results are shown.

KEY WORDS

Computer Vision, Plane Detection, Affine Homography

1 Introduction

Planes are important geometric features and can be used in a wide range of computer vision applications like vision based robot navigation [1] and camera calibration [2]. Planar surfaces present within a scene can provide useful information on the environment. A pair of images captured by a stereo rig or a single moving camera can be used to extract such information.

A wide range related to plane detection are found in the literature [3,4]. In [5], the normal vector to a plane is estimated by using only three corresponding points from stereo images. A method for detecting multiple planar regions using a progressive voting procedure from the solution of a linear system exploiting the two-view geometry is presented in [6]. SIFT (Scale Invariant Feature Transform) features were used in [7] to obtain the estimates of the planar homographies which represent the motion of the major planes in the scene. They track a combined Harris and SIFT features using the prediction by these homographies. The approach presented in [1] detects three-dimensional planar surfaces using 3D Hough transformation to extract plane segment candidates. Finally, a detailed review and performance comparisons of planar homography estimation techniques can be found in [8].

This work presents a homography-based method to detect and cluster planes using the affine model. The affine model was chosen because of its simplicity and because it allows good results. Using two image frames from a monocular sequence, a set of matched pairs of points is required in order to estimate all planar homographies. Each affine homography represents a planar surface present in the scene. A matching process is performed to obtain this set using a Harris corner detector combined with a local descriptor. We use SIFT as local descriptor. An algorithm was developed to cluster interest points belonging to the same plane. Tests are performed in different sequences of indoor and outdoor images. Results are illustrated showing the detected planes and validating the proposed method.

The paper is organized as follows. Section 2 presents some aspects related to planar homographies, highlighting the affine model. In Section 3, the proposed approach is formulated and in Section 4 the results are shown and discussed. Finally, Section 5 summarizes this work and some references are presented.

2 Planar Homography

When a planar object is imaged from multiple viewpoints the images are related by a unique homography. Given two views of the same plane $\pi = \begin{bmatrix}\mathbf{v}^T & 1\end{bmatrix}^T$, the ray corresponding to a point **x** in the image **I** meets the plane at a point $\mathbf{X}_\pi$, which projects into **x'** in image **I'**. The map from **x** to **x'** is the homography induced by the plane π. This is shown in Figure 1. Therefore, the homography is determined uniquely by the plane and vice versa [9].

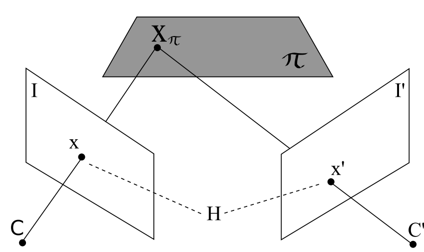

Figure 1: Given a planar object imaged from two viewpoints, the planar homography **H** is a mapping from points **x** of image **I** to points **x'** of image **I'**.

Given the projection matrices $\mathbf{P} = \begin{bmatrix}\mathbf{I}|0\end{bmatrix}^T$ and $\mathbf{P'} = \begin{bmatrix}\mathbf{A}|\mathbf{a}\end{bmatrix}^T$ for the two views, the homography induced by the plane is given by Equation 1.

$$\mathbf{x'} = \mathbf{H}\mathbf{x}, \tag{1}$$

with

$$\mathbf{H} = \mathbf{A} - \mathbf{a}\mathbf{v}^T$$

In Equation 1 **x** and **x'** are points in homogeneous coordinates. Therefore matrix **H** has 9 entries, but is defined only up to scale, so the number of degrees of freedom in a 2D projective transformation is 8. Each corresponding 2D point generates two constraints on **H** by Equation 1 and hence the correspondence of four points is sufficient to compute **H**.

2.1 Affine homography

An affine homography $\mathbf{H}_A$ can be defined as non-singular linear transformation followed by a translation. The matrix representation is formulated as in Equation 2

$$\begin{bmatrix} x' \\ y' \\ 1 \end{bmatrix} = \begin{bmatrix} a_{11} & a_{12} & t_x \\ a_{21} & a_{22} & t_y \\ 0 & 0 & 1 \end{bmatrix} \cdot \begin{bmatrix} x \\ y \\ 1 \end{bmatrix} \tag{2}$$

or in block form as in Equation 3

$$\mathbf{x'} = \mathbf{H}_A\mathbf{x} = \begin{bmatrix} \mathbf{A} & \mathbf{t} \\ \mathbf{0}^T & 1 \end{bmatrix} \cdot \mathbf{x}. \tag{3}$$

A planar affine homography has 6 degrees of freedom corresponding to the 6 matrix entries. Thus, the transformation can be computed from three point correspondences, i. e., the homography $\mathbf{H}_A$ can be computed from 3 matched pairs of points obtained using a pair of images captured by a stereo rig or a moving camera (monocular vision).

A modified version of *Direct Linear Transformation* method is used to estimate the homography. The last row of an affine homography $\mathbf{H}_A$ is equal to $\begin{bmatrix} 0 & 0 & 1 \end{bmatrix}$, thus Equation 1 can be formulated in terms of an inhomogeneous set of linear equations as Equation 4

$$\begin{bmatrix} x_1 & y_1 & 1 & 0 & 0 & 0 \\ 0 & 0 & 0 & x_1 & y_1 & 1 \\ x_2 & y_2 & 1 & 0 & 0 & 0 \\ 0 & 0 & 0 & x_2 & y_2 & 1 \\ x_3 & y_3 & 1 & 0 & 0 & 0 \\ 0 & 0 & 0 & x_3 & y_3 & 1 \end{bmatrix} \cdot \begin{bmatrix} h_1 \\ h_2 \\ h_3 \\ h_4 \\ h_5 \\ h_6 \end{bmatrix} = \begin{bmatrix} x'_1 \\ y'_1 \\ x'_2 \\ y'_2 \\ x'_3 \\ y'_3 \end{bmatrix}, \tag{4}$$

or in block form

$$\mathbf{X} \cdot \mathbf{H}_A = \mathbf{X'}, \tag{5}$$

where $\mathbf{x}_i = \begin{bmatrix} x_i & y_i \end{bmatrix}$ and $\mathbf{x'}_i = \begin{bmatrix} x'_i & y'_i \end{bmatrix}$ are the matched pairs of points in inhomogeneous coordinates and $\mathbf{H}_A$ has the form of Equation 6

$$\mathbf{H}_A = \begin{bmatrix} h_1 & h_2 & h_3 \\ h_4 & h_5 & h_6 \\ 0 & 0 & 1 \end{bmatrix}. \tag{6}$$

To estimate $\mathbf{H}_A$ from 3 matched pairs of points $\mathbf{x}_i \leftrightarrow \mathbf{x'}_i$, $i = 1, 2, 3$, we can solve the Equation 5 using the pseudo-inverse as

$$\mathbf{H}_A = (\mathbf{X}^T\mathbf{X})^{-1} \cdot \mathbf{X}^T\mathbf{X'} \tag{7}$$

whose computation is fast due to the low matrix dimensions.

2.2 Reprojection error

After an affine homography $\mathbf{H}_A$ has been computed, an error measure can be considered in order to verify whether a given matched pair of points belongs to the plane represented by $\mathbf{H}_A$. We use the *reprojection error* which can be defined as

$$e_i = |\mathbf{x}_i - \hat{\mathbf{x}}_i|^2 + |\mathbf{x'}_i - \hat{\mathbf{x}}'_i|^2, \tag{8}$$

where $\hat{\mathbf{x}}'_i = \mathbf{H}_A\mathbf{x}$ and $\hat{\mathbf{x}}_i = \mathbf{H}_A^{-1}\mathbf{x'}$.

When the reprojection error e_i is below a certain threshold, we consider that the given matched pair $\mathbf{x}_i \leftrightarrow \mathbf{x'}_i$ belongs to the plane represented by $\mathbf{H}_A$.

3 Plane Detection

A plane detection method is presented in this section. Interest points are detected using the Harris corner detector [10] in two acquired images (stereo rig or monocular sequence), and a set of corresponding points between these images are created using a local descriptor like SIFT [11]. After this step the Delaunay triangulation is performed on the set of interest points of the first image. Using the set of triangles resulting from the Delaunay method, a filtering scheme is applied to discard degenerate triangles. From this new set of triangles and the set of matched pairs of points from the combined Harris detector and SIFT descriptor, we compute the homographies and perform a clustering scheme to detect planes present in the imaged scene.

The entire methodology used is described in the following sections.

3.1 Interest points detection

Different primitives to detect and match image points exist in the literature [12]. The Harris corner detector was chosen since it is fast, reliable and provides good repeatability under varying rotation and illumination. The Harris' method is based on the computation of a matrix, M, using the partial derivatives of the intensity function

$$M = w \otimes \begin{pmatrix} \left(\frac{\partial I}{\partial x}\right)^2 & \left(\frac{\partial I}{\partial x}\right) \cdot \left(\frac{\partial I}{\partial y}\right) \\ \left(\frac{\partial I}{\partial x}\right) \cdot \left(\frac{\partial I}{\partial y}\right) & \left(\frac{\partial I}{\partial y}\right)^2 \end{pmatrix}, \tag{9}$$

where w specifies a gaussian window.

A corner is detected thresholding a measure based on the determinant and trace of matrix M (equation 9).

$$\begin{aligned} M &= \begin{pmatrix} A & C \\ C & B \end{pmatrix} \\ det(M) &= AB - C^2 \\ trace(M) &= A + B \\ R &= det(M) - k(trace(M))^2 \end{aligned} \tag{10}$$

where k is constant and empirically adjustable, and R is called *corner response*. Points with R above a certain threshold T_h are considered a corner. In order to eliminate weak corners a non-maximal suppression procedure is performed in the neighborhood of a detected corner.

3.2 Local descriptor

Following the detection of interest points in two consecutive images, a local descriptor must be used to establish a measure of correlation between the possible candidates to a matched pair of corners. This work uses the Scale Invariant Feature Transform descriptor. The combination of Harris detector with the SIFT descriptor can be considered as a good choice because it produces good, fast and stable results [13].

The SIFT descriptor is a local descriptor highly distinctive and invariant to changes in illumination and 3D viewpoint. The descriptor is based on the gradient magnitude and orientation of all pixels in a region around the keypoint. These are weighted by a gaussian window and accumulated into orientation histograms summarizing the contents over subregions, as shown in Figure 2. The length of each arrow corresponds to the sum of the gradient magnitudes near that direction within the region.

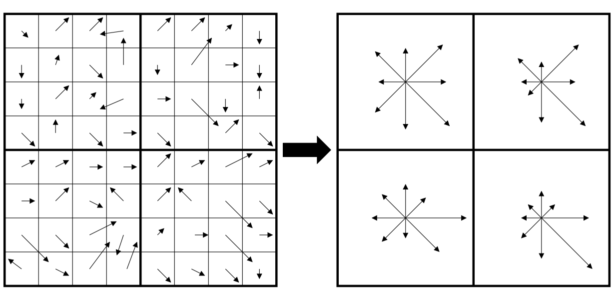

Figure 2: This figure shows a 2×2 descriptor array computed from an 8×8 set of samples. Each descriptor has 8 bins. The descriptor is represented by a vector of size 32 ($2 \times 2 \times 8$).

The orientation histogram entries corresponding to the lengths of the arrows is in the bottom of Figure 2. The descriptor is formed by a vector containing all these entries.

The distance between histograms (SIFT descriptor) is used as measure of correlation. A simple Euclidean measure of distance is used. If the distance is below a certain threshold then a possible matched pair is detected.

3.3 Regressive corner filtering and matching

A regressive filtering scheme is used to establish a correspondence between the detected corners to find matched pairs.

For each detected corner in the first image, a correspondent corner is searched for in a neighborhood in the second image satisfying a correlation measure described in Section 3.2. All corners in the first image, which do not have a correspondent in the second image are discarded. In the next step, a regressive filtering is performed to prevent that two or more corners of the first image have the same match in the second image. Now, for every corner in the second image 2, only the best correlated corner in the first image is maintained. At the end of the filtering, a set of matched pairs of corners M is obtained from the two images.

Given M, a Delaunay triangulation is performed only on the detected corners of the first image. Since the set of triangles has been obtained, a filtering scheme is applied to discard triangles that probably belong to virtual planes in the image. Only triangles with all sides within a certain range of lengths are considered valid. Still triangles with valid sides can have their vertices almost collinear. Collinearity of the three points used in the computation of the affine homographies must be avoided. To solve this problem, triangles with areas less than a certain value are also discarded. An example of Delaunay triangulation and filtering scheme applied to an indoor image frame is shown in Figure 3.

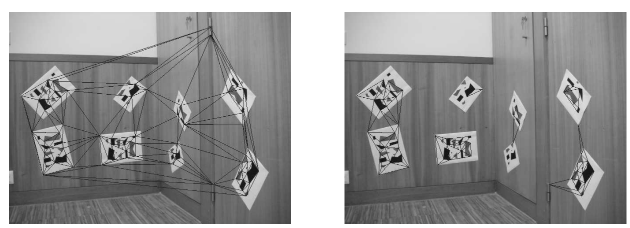

(a) Delaunay triangulation (b) Result from triangle filtering

Figure 3: Example of Delaunay triangulation and triangle filtering performed in indoor images.

The next step consists on a clustering scheme. The new set of triangles T obtained from the filtering scheme is used in a voting procedure to join points belonging to the same plane in the image. This is explained in the following section.

3.4 Clustering points

The clustering scheme consists of a voting procedure based on an affine homography and on the reprojection error, allowing obtaining planes and joining points in the same plane. At the end of this phase, each plane (cluster) is represented by an affine homography and planes with a small number of votes (points) are discarded. This procedure is detailed next.

Given the set of matched points M and the set of filtered Delaunay triangles T, we define H_p as the set of all p homographies existing between the two images. Each homography in H_p defines a plane in the image. Initially H_p is considered as empty. The first affine homography $\mathbf{H}_A$ is computed using the three points of the first triangle $T(1)$ and their matched pairs in the set M according to the Equation 7. Homography $\mathbf{H}_A$ thus obtained is included in H_p, and all used points are marked as *visited* and assigned to the homography $H_p(1)$, i.e., the first plane.

In the next step, the next triangle of T and their matched points in M is considered. For each $H_p(i)$ in H_p, all points of the triangle are checked to determine whether they belong to any of the existing planes in H_p. If the point had been marked as *not-visited* and the reprojection error for H_i is below a certain threshold, the point is marked as *visited* and assigned to homography H_i. If the point had been marked as *visited* and if the new reprojection error for H_i is smaller than the previous one, the point is assigned to plane H_i. In the case where all points of the triangle do not belong to any existing plane, a new affine homography $\mathbf{H}_A$ is computed with those points. The new homography represents a new plane and is included in H_p. This loop is performed until there are no unvisited matched pairs of points.

The clustering method described before can be described in the Algorithm 1.

At the end of clustering stage, only planes with a number of points above a certain threshold are considered.

Algorithm 1 Clustering coplanar points.

1 Create an empty set of homographies H_p
2 M: set of matched points between two images
4 T: set of triangles of the first image
5 t: number of triangles in T
6 err: reprojection error
7 T_e: reprojection error threshold
Take M and $T(1)$, compute $\mathbf{H}_A$ and put in H_p
Assigned the three points of the triangle $T(1)$ to $H_p(1)$, and mark them as *visited*
for $j = 2 : t$ **do**
  for i = each one in H_p **do**
    for each point p of $T(j)$ **do**
      if p = *not-visited* **then**
        if err < T_e **then**
          Assign p to $H_p(i)$
          Mark p as *visited*
        end if
      else if p = *visited* **then**
        if err < err_{old} **then**
          Update p to $H_p(i)$
        end if
      end if
    end for
  end for
  if All p of $T(j)$ = *not-visited* **then**
    Compute new $\mathbf{H}_A$ and put in H_p
    Assign all p to the new $\mathbf{H}_A$ and mark them as *visited*
  end if
end for

4 Experimental Results

In this section we report experiments that demonstrate accurate plane detection from two consecutive frames of an image sequence. Four image sequences of different outdoor scenes were acquired by a camera. All used images in the experiments are in gray level with size 640×480.

Different parameters were empirically adjusted at each stage of the entire process of plane detection. The following sections discuss each one of them.

4.1 Interest point detection

At this stage, the Harris detector was implemented using $k = 0.13$ and a gaussian window with standard deviation $\sigma = 1.5$ and size of $6\sigma \times 6\sigma$. A threshold value T_h was used to distinguish between corners and non-corners. T_h must be set high enough to avoid the detection of false corners which may have a relatively large corner response R (Equation 10) due to noise. The value of T_h is based on the maximum corner response computed, R_{max}. It was used $T_h = 0.01 \cdot R_{max}$. After all corners had been detected, a non-maximum suppression scheme was performed with a window of size 10×10, in order to eliminate weak corners.

4.2 Local descriptor

The best results were obtained using SIFT with 4×4 descriptors computed from a 16×16 sample array. The weighting gaussian window has size 16×16 and $\sigma = 1.5$. Each descriptor is described by an orientation histogram with 8 bins, each one of size $\pi/4$. The total size of SIFT descriptor is 128 ($4 \times 4 \times 8$).

A simple Euclidean distance d was used to compare descriptors. If $d < T_m$ then we have a possible matched pair of interest points. It was initialized $T_m = 10$.

4.3 Regressive corner filtering and matching

In the regressive corner filtering and matching stage, we must perform a search in the second image for a corner that best matches a specific corner in the first image. This should be done for all detected corners in the first image. The size of the region of search can be constrained to improve the computational efficiency of the algorithm. This region can be defined based on the largest displacement of pixel, i.e., based on the camera's movement during the acquisition process. In our case a region around the interest point of size 25×25 was used.

The value of T_m is dynamically adjusted during the process of matching. When a possible match is found, the value of the threshold T_m is updated with the computed distance d. This was done to allow that the best candidate is chosen as a match.

As explained in Section 3.3, Delaunay triangulation is performed, followed by triangle filtering. Only triangles with sides of length between 5 and 80 pixels, and area over 10 pixels $\times$ pixels, are considered as valid.

4.4 Clustering points

Only one parameter is adjustable at this stage. A reprojection error threshold was empirically chosen as $T_e = 3.0$. The value of T_e is dynamically updated during the clustering process. Thus, each matched pair of points in the set M is assigned to the best homography in the set H_p based on the computed reprojection error.

4.5 Results

Many different sequences were used in the experiments. Due to paper size restrictions only few results are shown here. Sequences with planes at different positions and orientations in the scene were chosen.

The planes detected are shown using geometric markers in the first frame of each sequence. The results for outdoor sequences are shown in Figures 4, 5 and 6.

Figure 4: Detected planar regions in outdoor sequence 1.

The results for indoor sequences are shown in Figures 7, 8 and 9.

4.6 Discussion

The sequences were acquired under different conditions of illumination and different positions of the camera relative to the planes in the scene. The best results were obtained using Harris corner detector combined with SIFT descriptor in the matching process.

The matching process is one of the most important stages of the algorithm. An important parameter is the size of the region in which a match is searched for.

Figure 5: Detected planar regions in outdoor sequence 2.

Figure 6: Detected planar regions in outdoor sequence 3.

Each one of the image sequences used in the experiments presents two major planes of a scene. In some cases of indoor scenes, more than two planes were detected (Figure 8. The results clearly show that the algorithm performs well using indoor and outdoor images.

5 Conclusion

In this paper we present a homography-based method for detecting planes. The affine model was chosen for its simplicity. In order to obtain a set of matched points between two frames of an image sequence, the Harris corner detector combined with SIFT descriptor and a regressive filtering method was used. Delaunay triangulation was performed on the set of corners of the first image frame. In order to avoid degenerate configurations in the estimation of the affine homographies, a triangle filtering scheme was used to discard triangles that would likely represent virtual planes.

The algorithm was tested using outdoor image sequences and presented good results. Future work will be concentrated at combining affine homography and affine optical flow to improve the precision and reliability under a wide range of conditions.

Figure 7: Detected planar regions in indoor sequence 1.

Figure 8: Detected planar regions in indoor sequence 2.

Figure 9: Detected planar regions in indoor sequence 3.

Acknowledgements

This work is partially supported by the CAPES Foundation under grant no. 1087/07-0.

6 References

[1] K. Okada, S. Kagami, M. Inaba and H. Inoue, Plane segment finder: algorithm, implementation and applications, *Proc. IEEE Int. Conf. on Robotics and Automation*, Seoul, Korea, 2001, 2120-2125.

[2] P. F. Sturm and S. J. Maybank, On plane-based camera calibration: A general algorithm, singularities, applications, *Computer Vision and Pattern Recognition*, *1*, 1999, 432-437.

[3] D. Sinclair and A. Blake, Quantitative planar region detection, *Int. Journal of Computer Vision*, *18*(1), 1996, 77-91.

[4] Q. He, C-H. H. Chu, Planar surface detection in image pairs using homographic constraints, *Proc of Int. Symp. on Visual Computing*, Lake Tahoe, Nevada, USA, 2006, 19-27.

[5] J. Piazzi and D. Prattichizzo, Plane detection with stereo images, *Proc. of IEEE Int. Conf. on Robotics and Automation*, Orlando, Florida, USA, 2006, 922-927.

[6] G. Silveira, E. Malis and P. Rives, Real-time robust detection of planar regions in a pair of images, *Proc. of Int. Conf. on Intelligent Robots and Systems*, Beijing, China, 2006, 49-54.

[7] R. Rodrigo, Z. Chen and J. Samarabandu, Feature motion for monocular robot navigation, *Proc. of Int. Conf. on Information and Automation*, Colombo, Sri Lanka, 2006, 201-205.

[8] A. Agarwal, C. V. Jawahar and P. J. Narayanan, A survey of planar homography estimation techniques, Technical Report IIIT/TR/2005/12, Centre for Visual Information Technology, 2005.

[9] R. Hartley and A. Zisserman, *Multiple view geometry in computer vision* (Cambridge, UK: Cambridge University Press, 2004).

[10] C. Harris and M. Stephens, A combined corner and edge detection, *Proc. of 4th Alvey Vision Conference*, Manchester, UK, 1988, 147-152.

[11] D. Lowe, Distinctive image features from scale-invariant keypoints, *Int. Journal of Computer Vision*, *20*, 2003, 91-110.

[12] K. Mikolajczyk and C. Schmid, Scale and affine invariant interest point detectors, *Int. Journal of Computer Vision*, *60*(1), 2004, 63-86.

[13] K. Mikolajczyk and C. Schmid, A performance evaluation of local descriptors, *IEEE Trans. on Patt. Analysis & Machine Intelligence*, 27(10), 2005, 1615-1630.